J. Astrophys. Astr. (2018) 39:40
https://doi.org/10.1007/s12036-018-9533-6

Calculation of the transport coefficients of the nuclear pasta phase

RANA NANDI[1,*] and STEFAN SCHRAMM[2]

[1] Tata Institute of Fundamental Research, Mumbai 400 005, India.
[2]Frankfurt Institute for Advanced Studies, 60438 Frankfurt am Main, Germany.
*Corresponding author. E-mail: rana.nandi@tifr.res.in

MS received 31 May 2018; accepted 11 June 2018; published online 11 July 2018

Abstract. We calculate the transport coefficients of low-density nuclear matter, especially the nuclear pasta phase, using quantum molecular dynamics simulations. The shear viscosity as well as the thermal and electrical conductivities are determined by calculating the static structure factor of protons for all relevant density, temperature and proton fractions, using simulation data. It is found that all the transport coefficients have similar orders of magnitude as found earlier without considering the pasta phase. Our results are thus in contrast to the common belief that the pasta layer is highly resistive and therefore have important astrophysical consequences.

Keywords. Neutron stars—transport properties—molecular dynamics.

1. Introduction

Based on the composition a neutron star (NS) can be divided into several parts. At the surface there is a thin envelope containing mostly H and He ions and Fe atoms. The outer crust starts at $\sim 10^4$ g cm^{-3} when atoms get fully ionized and form a Coulomb lattice embedded in an electron gas. With increasing density the nucleus become increasingly neutron-rich due to electron capture process. At $\sim 4 \times 10^{11}$ g cm^{-3}, the nucleus become so neutron rich that neutrons begin to drip out of the nuclei (Baym *et al.* 1971; Rüster *et al.* 2006; Nandi & Bandyopadhyay 2011). This marks the end of the outer crust and the beginning of the inner crust. In the inner crust nuclei are immersed in both an electron gas and a neutron gas (Haensel 2001; Nandi *et al.* 2011). With further increase in density, nuclei come closer and at $\sim 10^{14}$ g cm^{-3} they merge together to form uniform matter of neutrons, protons, electrons and muons. Just before the transition to uniform matter, nuclei take various complicated shapes due to the competition between Coulomb energy and surface energy. These exotic shapes are collectively known as nuclear 'pasta phase' (Ravenhall *et al.* 1983).

The study of pasta phase is crucial to understand various astrophysical phenomena. For example, the scattering of neutrinos from the pasta phase in core-collapse supervovae can significantly affect the neutrino transport, that plays a critical role in the eventual supernova explosion (Horowitz *et al.* 2004). On the other hand, the electron-pasta scattering is supposed to greatly influence the transport properties like shear viscosity and thermal and electrical coductivities of NS crust and therefore, can play a crucial role in understanding the phenomena of cooling (Horowitz *et al.* 2015), magnetic field decay (Pons *et al.* 2013), crustal oscillations (Chugunov & Yakovlev 2005), etc. of NS.

The pasta phase was initially studied by static methods using few specific shapes (Ravenhall *et al.* 1983; Lorenz *et al.* 1993; Oyamatsu 1993; Newton & Stone 2009). However, since the shapes are not known *a priori* it is important to adopt dynamical approach that allows arbitrary nuclear shapes. After the first work of Maruyama *et al.* (1998), several authors have studied the characteristics of pasta phase using molecular dynamics simulation of different types (Horowitz *et al.* 2004; Schneider *et al.* 2013; Dorso *et al.* 2012; Watanabe *et al.* 2003; Nandi & Schramm 2016, 2017; Schramm & Nandi 2017a, b). In this article, we study the transport properties of the nuclear pasta phase using quantum molecular dynamics (QMD) simulation.

2. Formalism

In QMD, the wave function of a nucleon is represented by a Gaussian wave packet with time-independent width. The interaction between nucleons is described by

a Skyrme-like Hamiltonian (Nandi & Schramm 2018; Chikazumi *et al.* 2001)

$$\mathcal{H} = T + V_{\rm Pauli} + V_{\rm Skyrme} + V_{\rm sym} + V_{\rm MD} + V_{\rm Surface} + V_{\rm Coul}, \quad (1)$$

where T is the kinetic energy, $V_{\rm Pauli}$ is the phenomenological Pauli potential, $V_{\rm Skyrme}$ is the Skyrme-like interaction between nucleons, $V_{\rm MD}$ denotes the momentum-dependent part, $V_{\rm sym}$ is the isospin-dependent part, $V_{\rm Surface}$ is the potential that depends on the density gradient and $V_{\rm Coul}$ is the Coulomb interaction. The explicit expressions for all the potentials can be found in Nandi and Schramm (2018).

The dominant contribution to transport properties like shear viscosity (η) and thermal and electrical conductivities (κ, σ) of pasta phase comes from electron-ion scattering as electrons are the most important carriers of charge and momentum in this condition. All these transport coefficients can easily be calculated when the static structure factor ($S_{\rm p}(q)$) that describes correlation between protons is known. We calculate $S_{\rm p}(q)$ from the autocorrelation function (Nandi & Schramm 2018)

$$S_{\rm p}(q) = \frac{1}{N_{\rm p}} \langle \rho_{\rm p}(q,t)^* \rho_{\rm p}(q,t) \rangle, \quad (2)$$

where $\rho_{\rm p}(q,t)$ is the Fourier transform of proton number density, which is calculated using positions of the nucleons at time t. The average is taken over simulation time as well as all the directions of momentum transfer $\mathbf{q} = \frac{2\pi}{L}(l, m, n)$, where l, m, n are integers and L is the length of the cubic simulation box determined from the number of nucleons used in the simulation and the density as $L = (N/\rho)^{1/3}$. To incorporate long-range (small $\mathbf{q}$) correlations among protons one needs to have enough number of particles. We take 4096 nucleons at $\rho = 0.1\rho_0$ ($\rho_0 = 0.168$ fm^{-3} is the nuclear saturation density), and increase it with density keeping L fixed at 62.47 fm. Therefore, for the highest density ($0.6\rho_0$) considered here we have 24,576 particles. To keep the simulation runtime within reasonable limit, we perform simulation using GPU platform.

3. Results

We calculate $S_{\rm p}(q)$ and subsequently transport coefficients for various density, temperatures and proton fraction ($Y_{\rm p}$) relevant for various astrophysical scenarios. In Fig. 1, we plot $S_{\rm p}(q)$ as a function of q for symmetric nuclear matter at $\rho = 0.1\rho_0$ and temperatures $T = 1$–5 MeV. The $S_{\rm p}(q = q_{\rm peak})$ is proportional to the size of the clusters but get corrected by the nuclear form factor and the screening effects of other ions. At $\rho = 0.1\rho_0$, nucleons form spherical clusters. With increasing T more and more nucleons evaporate from clusters making the system increasingly uniform and hence lead to smaller $S_{\rm p}(q_{\rm peak})$. An interesting behavior of $S_{\rm p}(q)$ is seen in the pasta phase region ($\rho \gtrsim 0.2\rho_0$). In Fig. 2, we plot $S_{\rm p}(q)$ for asymmetric nuclear matter ($Y_{\rm p} = 0.3$) at $\rho = 0.4\rho_0$. From the figure, we see that $S_{\rm p}(q)$ increases very sharply at $T = 2$ MeV. This is because cylindrical structures found at this density at low T merge together to form almost perfect equidistant slabs at $T = 2$, as can be seen from the snapshot shown in Fig. 3. With further increase in T, these slabs gradually merge to form bubble phase and $S_{\rm p}(q)$ decreases, as a consequence. In Fig. 4, we plot $S_{\rm p}(q)$ for all density and temperatures considered here. A careful observation shows that at low-density $S_{\rm p}(q)$ decreases with temperature for all three values of $Y_{\rm p}$. However in the pasta phase region ($\rho \gtrsim 0.2\rho_0$), the

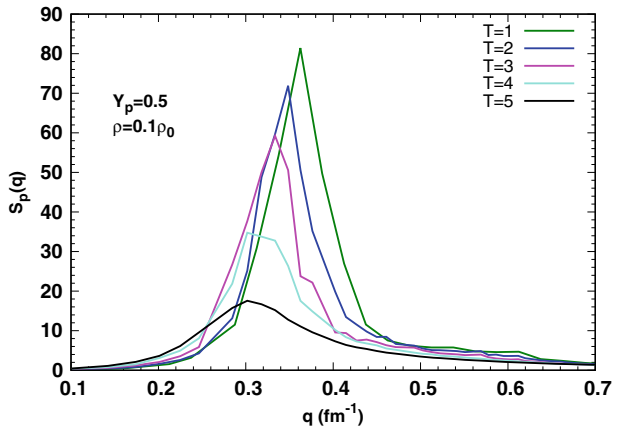

Figure 1. Static structure factor versus momentum transfer for protons at $\rho = 0.1\rho_0$, $Y_{\rm p} = 0.5$ and different temperatures ($T = 1$–5) MeV.

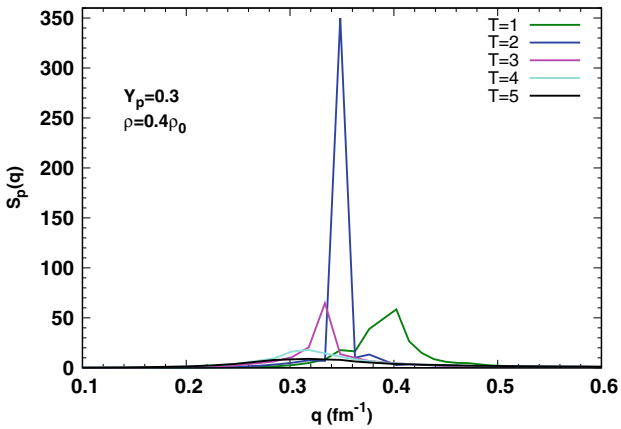

Figure 2. Same as in Fig. 1, but for $Y_{\rm p} = 0.3$ and $\rho = 0.4\rho_0$.

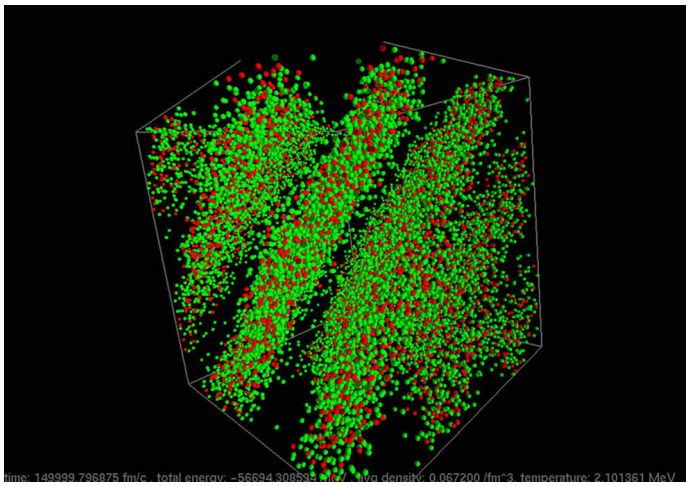

Figure 3. Simulation snapshot for neutron (green) and proton (red) distributions at $\rho = 0.4\rho_0$, $Y_\mathrm{p} = 0.3$ and $T = 2$ MeV.

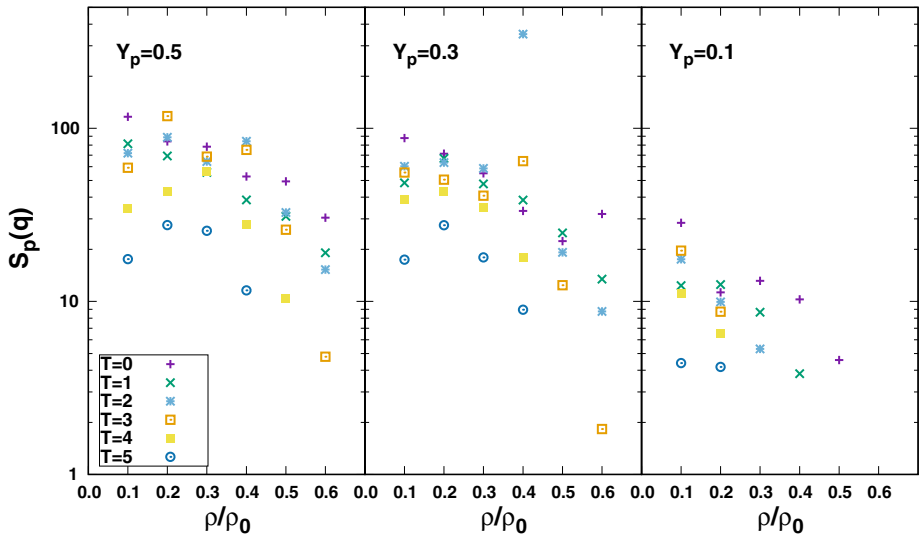

Figure 4. $S_\mathrm{p}(q)$ as a function of density for Y_p and T.

$S_\mathrm{p}(q)$ rises at intermediate temperatures as discussed before in connection to Fig. 2.

Using the calculated structure factors we finally calculate the transport coefficients. In Fig. 5 and Fig. 6, we display the results of shear viscosity and thermal conductivity for asymmetric nuclear matter with $Y_\mathrm{p} = 0.3$ and $Y_\mathrm{p} = 0.1$, which are typical values for supernova matter and neutron star inner crust, respectively. It is observed that although there are irregularities in the pasta phase region both the transport coefficients generally increase with density and temperature. Most importantly, the order of magnitude of both the coefficients are same as found earlier without considering the pasta phase (Flowers & Itoh 1976; Nandkumar & Pethick 1983). Similar behavior is also found for electrical conductivity.

4. Conclusion

We have calculated the transport coefficients namely shear viscosity and thermal and electrical conductivities of low-density nuclear matter at various astrophysical conditions, using quantum molecular dynamics simulations. Under these conditions the electrons are most important carriers and their transport is limited mainly by electron–ion scattering, which we calculate by determining the static structure for protons ($S_\mathrm{p}(q)$) using our simulation data. Although $S_\mathrm{p}(q)$ shows some irregularities in the pasta region, all the transport coefficients are found to have similar orders of magnitude as found without considering the pasta phase. Our results therefore contradict the speculation that the pasta layer is highly resistive and bear important astrophysical

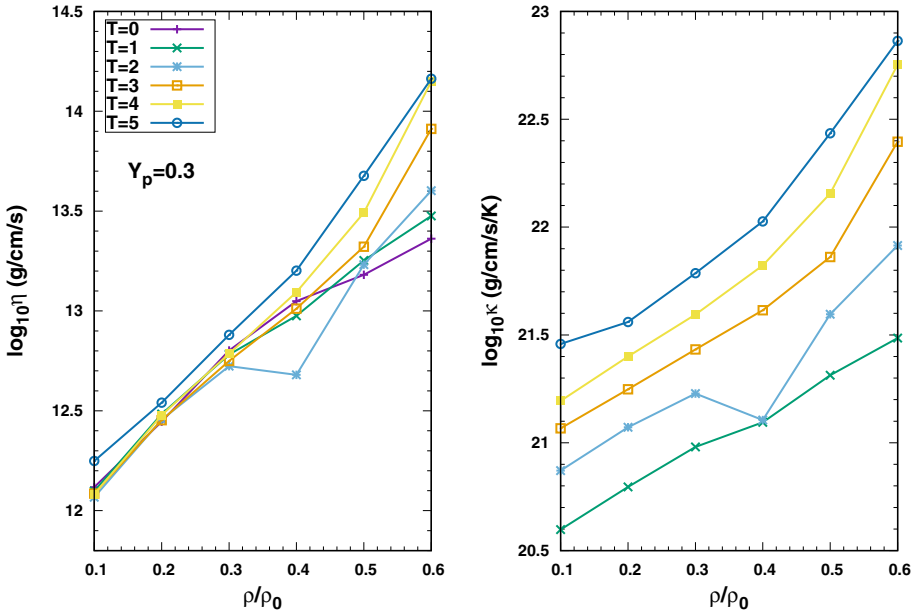

Figure 5. Shear viscosity and thermal conductivity of nuclear matter as a function of density and temperature at $Y_p = 0.3$.

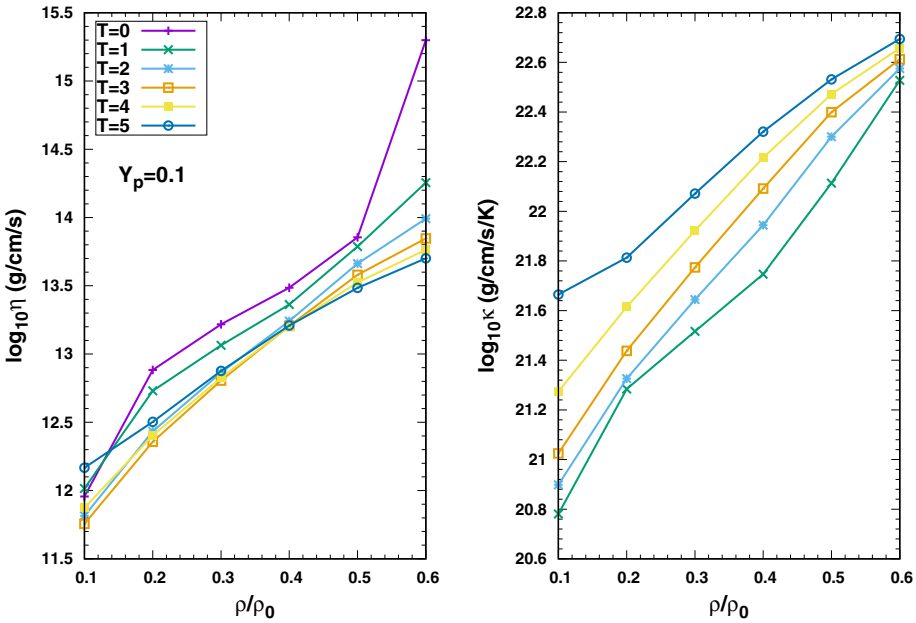

Figure 6. Same as in figure 5, but with $Y_p = 0.1$.

consequences. However, longer and larger simulations are required to confirm these findings.

References

Baym G., Pethick C., Sutherland P. 1971, Astrophys. J., 45, 429

Chikazumi S., Maruyama T., Chiba S., Niita K., Iwamoto A. 2001, Phys. Rev. C, 63, 024602

Chugunov A. I., Yakovlev D. G., 2005, Astron. Rep., 49, 724

Dorso C. O., Giménez Molinelli P. A., López J. A. 2012, Phys. Rev. C, 86, 055805

Flowers, E., Itoh, N. 1976, Astrophys. J., 206, 218

Haensel P. 2001, Physics of Neutron Star Interiors, Lecture Notes in Physics 578, Springer, Berlin, p. 127

Horowitz C. J., Pérez-García M. A., Piekarewicz J. 2004, Phys. Rev. C, 69, 045804

Horowitz C. J., Berry D. K., Briggs C. M., Caplan M. E., Cumming A., Schneider A. S. 2015, Phys. Rev. Lett., 114, 031102

Lorenz C. P., Ravenhall D. G., Pethick C. J. 1993, Phys. Rev. Lett., 70, 379
Maruyama T., Niita K., Oyamatsu K., Maruyama T., Chiba S., Iwamoto A. 1998, Phys. Rev. C, 57, 655
Nandkumar R., Pethick C. J. 1983, Mon. Not. R. Astron. Soc., 209, 511
Nandi R., Bandyopadhyay D., Mishustin I., Greiner W. 2011, Astrophys. J., 736, 156
Nandi R., Bandyopadhyay D. 2011, J. Phys. Conf. Ser., 312, 042016
Nandi R., Schramm S. 2016, Phys. Rev. C, 94, 025806
Nandi R., Schramm S. 2017, Phys. Rev. C, 95, 065801
Nandi R., Schramm S. 2018, Astrophys. J., 857, 12
Newton W. G., Stone J. R. 2009, Phys. Rev. C, 79, 055801
Oyamatsu K. 1993, Nucl. Phys., A561, 431
Pons J. A., Viganò D., Rea N. 2013, Nat. Phys., 9, 431
Ravenhall D. G., Pethick C. J., Wilson J. R. 1983, Phys. Rev. Lett., 50, 2066
Rüster S. B., Hempel M., Schaffner-Bielich J. 2006, Phys. Rev. C, 73, 035804
Schneider A. S., Horowitz C. J., Hughto J., Berry D. K. 2013, Phys. Rev. C, 88, 065807
Schramm S., Nandi R. 2017a, J. Phys. Conf. Ser., 861, 012021
Schramm S., Nandi R. 2017b, Int. J. Mod. Phys. Conf. Ser., 45, 1760027
Watanabe G., Sato K., Yasuoka K., Ebisuzaki T. 2003, Phys. Rev. C, 68, 035806